Response to Comments of Reviewer #2

Manuscript number: acp-2024-3470
Title: Effects of 2010-2045 climate change on ozone levels in China under carbon neutrality scenario: Key meteorological parameters and processes

General comments: This study investigates the impact of 2010-2045 climate changes on the ozone levels under carbon neutrality scenario using the GISS-E2.1 GCM and the GEOS-Chem models. The results of this study have important implication to the future air pollution control strategy development. The paper is well written. I recommend its acceptance for publication after some minor revisions.

Thanks to the referee for the helpful comments and constructive suggestions. We have revised the manuscript carefully and the point-to-point responses are listed below.

Major concerns/questions:

1. Line 52-53: It is a 33% reduction in 90th MDA8 O_3, rather than 84%.

Response:

Thanks for pointing this out. We have changed "84%" to "33%".

2. Line 151-154: A detailed description about the SSPs inventory is suggested. For the present-day anthropogenic emissions (year 2015), the MEIC inventory is more widely used to drive air quality models in China. What is the different in various pollutant emissions between SSPs and MEIC emission inventories for the year 2015? Moreover, for the future biomass burning emission inventory, how is it developed? If wild fire emissions are included, is it considered the impact of future climate changes?

Response:

Description of SSPs inventory is presented in the second paragraph of "Introduction" section: "Shared Socioeconomic Pathways (SSPs) are the state-of-the-art global emission scenarios, which combines socioeconomic and technological development with future climate radiative forcing outcomes (RCPs) into a scenario matrix architecture (Gidden et al., 2019). Gidden et al. (2019) constructed nine scenarios of future emissions trajectories, including SSP1-1.9, SSP1-2.6, SSP2-4.5, SSP3-7.0, SSP3-LowNTCF, SSP4-3.4, SSP4-6.0, SSP5-3.4-Overshoot (OS), and SSP5-8.5. Among all scenarios, only the SSP1-1.9 scenario achieves net negative emissions of carbon dioxide (CO2) for China and the world by 2060 (Wang et al., 2023), and thus we defined it as the carbon neutrality scenario and applied in this work."

To make it more detailed, we have added the following sentences in the first paragraph of Section 2.2.2: "Global anthropogenic and biomass burning emissions of pollutants are from the SSP1-1.9 inventory, which has a monthly temporal resolution and a 0.5° spatial resolution. The anthropogenic emissions in SSPs are from nine sectors (including agricultural, energy, industry, transportation, residential and commercial, solvents production and application, waste, international shipping, and aircraft), and the biomass burning emissions are from four sectors (including agricultural waste burning, forest burning, grassland burning, and peat burning) (Gidden et al., 2019). Future anthropogenic and biomass burning emission are obtained from the integrated assessment model (IAMs) results for each SSPs scenario after harmonization (enabling consistent transitions from the historical data used in CMIP6 to future trajectories) and downscaling (improving the spatial resolution of emissions) (Gidden et al., 2019). The impacts of future climate change on biomass burning emissions (including wild fire emissions) are not considered.".

The annual total anthropogenic emissions of NO_x, CO, NMVOCs, SO_2, NH_3, OC, and BC over China in 2015 are 33.6, 190.0, 30.0, 24.8, 13.0, 5.2, and 2.6 Tg yr^{-1} for SSP1-1.9 inventory (Gidden et al., 2019), respectively, and those are 23.7, 153.6, 28.5, 16.9, 10.5, 2.5, and 1.5 Tg yr^{-1} for MEIC inventory (Zheng et al., 2018), respectively. The annual emissions of all pollutants over China in the SSP1-1.9 are higher than in the MEIC. However, compared with observations, the simulated seasonal mean MDA8 O_3 concentrations from the GEOS-Chem model with SSP1-1.9 inventory

have NMBs of 7.1-12.1% (Fig. 3), indicating that the model can capture fairly well the observations in China in 2015.

3. Line 360-361: The vertical profiles of present-day seasonal mean O_3 mass are shown in Figure S2, but not Figure 8.

Response:

Figure 8a shows the vertical profiles of present-day seasonal mean O_3 mass (Gg d^{-1}) for five processes (including net chemical production, PBL mixing, dry deposition, cloud convection, and horizontal and vertical advection transport), while Figure S2 shows the vertical profiles of present-day seasonal mean O_3 concentrations (ppbv). Therefore, the statement in text is correct.

4. The citation of figures and sections in texts should be carefully checked. For example, "Figure S3" should be "Figure S2" in Line 369; "Sect. 5.1" should be "Sect. 3.3.1".

Response:

Thanks for pointing this out. We carefully checked the citation of figures and sections in texts, and corrected the errors.

5. Figure S6: The tropospheric columns of NO_2 seem to be significantly overestimated by the models compared with the OMI satellite data. Reasonable attributions should be given and its impact on the FNR analysis should be discussed. Is it due to the uncertainties in the SSPs inventory? Besides, validations of simulated NO_2 near surfaces like Figure S1 using the surface measurements are suggested.

Response:

There are several possible reasons for the overestimation of tropospheric NO_2 columns in GCAP 2.0 simulation. Firstly, the uncertainties in the OMI products. Shah et al. (2020) reported that the GEOS-Chem tends to overestimate tropospheric NO_2 columns compared to the European Quality Assurance for Essential Climate Variables (QA4ECV) retrieval product (used in this work) (Boersma et al., 2018), owing to the strong sensitivity of the vertical distribution of NO_2 to that of aerosols and the misclassification of polluted scenes with high aerosol optical depth (and likely high NO_2) as clouds in QA4ECV retrieval. Secondly, SSP1-1.9 has higher NO_x emissions in 2015 compared to MEIC. Finally, the inconsistencies in the sampling time. The GEOS-Chem model in this work only outputs the daily NO_2 values, while the overpass time of OMI satellite is about 13:45 local time. The observed tropospheric NO_2 column around 13:45 by Geostationary Environment Monitoring Spectrometer (GEMS) geostationary satellite was generally lower than the daily mean from the GEOS-Chem in Beijing for DJF 2021/22 and JJA 2022 (Yang et al., 2024).

To evaluate the impacts of this overestimation on the FNR analysis, we have examined the distributions of seasonal mean FNR over EC in 2015 from both the model and OMI observations (Figure R1 below). Compared to the model results, the observed VOC-limited regime shrinks toward the NCP and its surrounding areas in DJF, MAM, and SON, and in these seasons decreases in anthropogenic emissions increase MDA8 O_3 concentrations. As a result, the uncertainties in FNR do not affect our analysis of the effects of future emission changes (Figure 4).

Following the Reviewer's suggestion, we have added Figure S8 in the Supplementary Material to evaluate the model performance for surface NO_2. We have also added the following sentences in the S1 of Supplementary Material to describe the model performance: "We also compared the simulated surface NO_2 concentrations with observations from CNEMC in Fig. S8. The model generally captured the observed monthly variation in surface NO_2 concentrations in EC, NCP, and YRD, with R values of 0.44-0.70. The systematic low biases of surface NO_2 concentrations in the GEOS-Chem model (NMBs ranging from -51.7% to -19.2% in this work) were also reported in previous studies (Qu et al., 2020; Qu et al., 2022; Fang et al., 2024), because of the lack of representation of the spatial gradients in NO_2 observations within the coarse GEOS-Chem grid cells (Qu et al., 2022).".

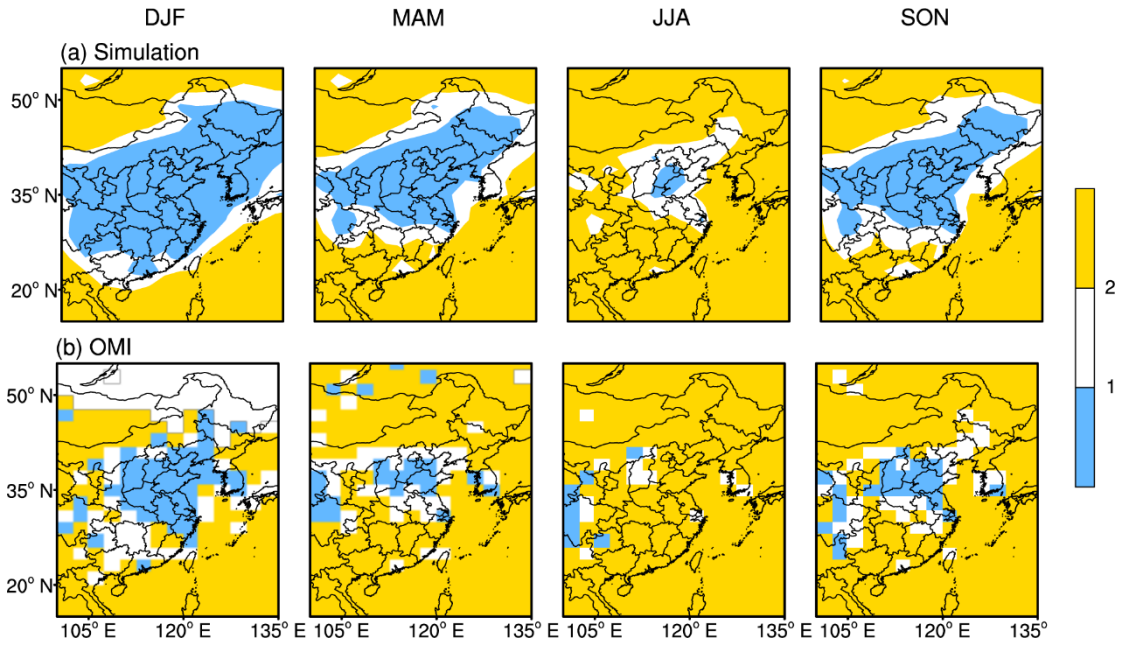

Figure R1. Distributions of seasonal mean formaldehyde nitrogen ratio (FNR) over EC in 2015 from (a) the model and (b) the OMI observations.

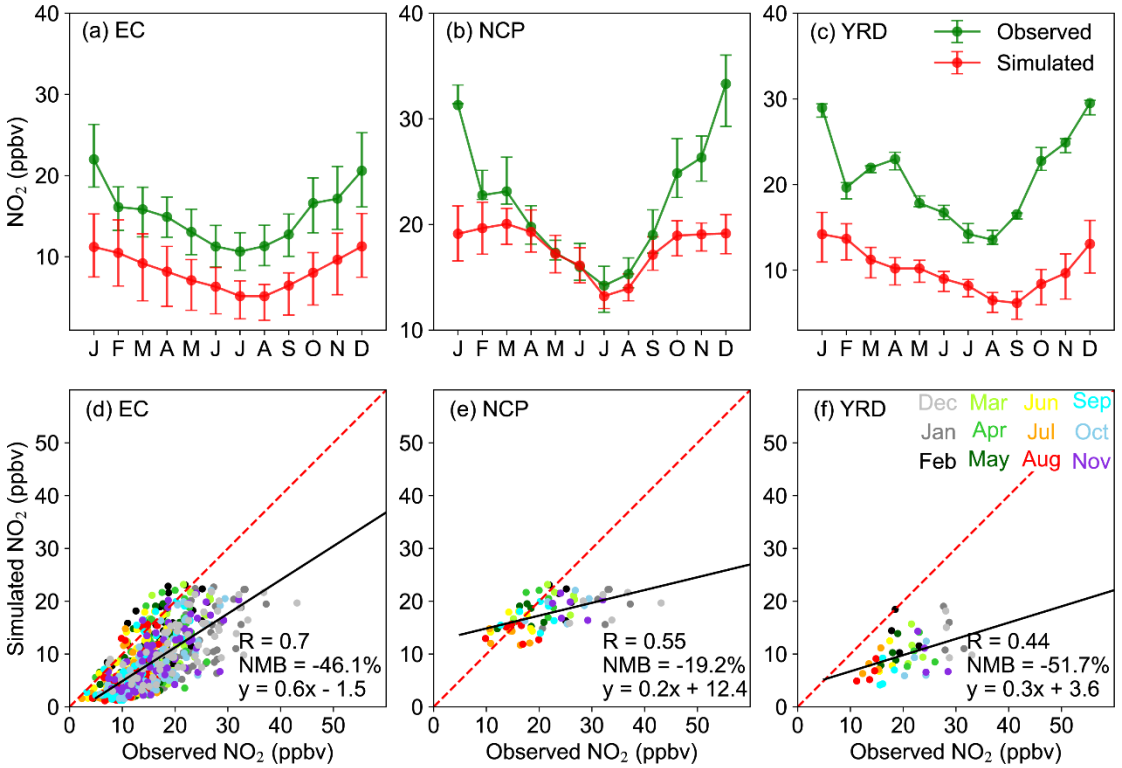

Figure S8. (a)-(c) Monthly variations in simulated and observed surface NO_2 concentrations (ppbv) over (a) EC (with a total of 68 grids), (b) NCP (with a total of 6 grids), and (c) YRD (with a total of 4 grids) regions. Bars represent the range from first to third quartiles of all grid samples in this region. (d)-(f) The scatterplot of simulated versus observed monthly mean surface NO_2 concentrations for grids in EC, NCP, and YRD. The linear fit (black solid line and equation), correlation coefficient (R), and normalized mean biases (NMB) that calculated for grids in these three regions are also shown when all of the year 2015 data are considered.

References:

Boersma, K. F., Eskes, H. J., Richter, A., De Smedt, I., Lorente, A., Beirle, S., van Geffen, J. H. G. M., Zara, M., Peters, E., Van Roozendael, M., Wagner, T., Maasakkers, J. D., van der A, R. J., Nightingale, J., De Rudder, A., Irie, H., Pinardi, G., Lambert, J.-C., and Compernolle, S. C.: Improving algorithms and uncertainty estimates for satellite NO_2 retrievals: results from the quality assurance for the essential climate variables (QA4ECV) project, Atmos. Meas. Tech., 11, 6651-6678, https://doi.org/10.5194/amt-11-6651-2018, 2018.

Fang, L., Jin, J., Segers, A., Li, K., Xia, J., Han, W., Li, B., Lin, H. X., Zhu, L., Liu, S., and Liao, H.: Observational operator for fair model evaluation with ground NO_2 measurements, Geosci. Model Dev., 17, 8267-8282, https://doi.org/10.5194/gmd-17-8267-2024, 2024.

Gidden, M. J., Riahi, K., Smith, S. J., Fujimori, S., Luderer, G., Kriegler, E., van Vuuren, D. P., van den Berg, M., Feng, L., Klein, D., Calvin, K., Doelman, J. C., Frank, S., Fricko, O., Harmsen, M., Hasegawa, T., Havlik, P., Hilaire, J., Hoesly, R., Horing, J., Popp, A., Stehfest, E., and Takahashi, K.: Global emissions pathways under different socioeconomic scenarios for use in CMIP6: a dataset of harmonized emissions trajectories through the end of the century, Geosci. Model Dev., 12, 1443-1475, https://doi.org/10.5194/gmd-12-1443-2019, 2019.

Qu, Z., Henze, D. K., Cooper, O. R., and Neu, J. L.: Impacts of global NO_x inversions on NO_2 and ozone simulations, Atmos. Chem. Phys., 20, 13109-13130, https://doi.org/10.5194/acp-20-13109-2020, 2020.

Qu, Z., Henze, D. K., Worden, H. M., Jiang, Z., Gaubert, B., Theys, N., and Wang, W.: Sector-Based Top-Down Estimates of NO_x, SO_2, and CO Emissions in East Asia, Geophys. Res. Lett., 49, https://doi.org/10.1029/2021gl096009, 2022.

Shah, V., Jacob, D. J., Li, K., Silvern, R. F., Zhai, S., Liu, M., Lin, J., and Zhang, Q.: Effect of changing NO_x lifetime on the seasonality and long-term trends of satellite-observed tropospheric NO_2 columns over China, Atmos. Chem. Phys., 20, 1483-1495, https://doi.org/10.5194/acp-20-1483-2020, 2020.

Wang, Y., Liao, H., Chen, H., and Chen, L.: Future Projection of Mortality From Exposure to $PM_{2.5}$ and O_3 Under the Carbon Neutral Pathway: Roles of Changing Emissions and Population Aging, Geophys. Res. Lett., 50, https://doi.org/10.1029/2023gl104838, 2023.

Yang, L. H., Jacob, D. J., Dang, R., Oak, Y. J., Lin, H., Kim, J., Zhai, S., Colombi, N. K., Pendergrass, D. C., Beaudry, E., Shah, V., Feng, X., Yantosca, R. M., Chong, H., Park, J., Lee, H., Lee, W.-J., Kim, S., Kim, E., Travis, K. R., Crawford, J. H., and Liao, H.: Interpreting Geostationary Environment Monitoring Spectrometer (GEMS) geostationary satellite observations of the diurnal variation in nitrogen dioxide (NO_2) over East Asia, Atmos. Chem. Phys., 24, 7027-7039, https://doi.org/10.5194/acp-24-7027-2024, 2024.

Zheng, B., Tong, D., Li, M., Liu, F., Hong, C., Geng, G., Li, H., Li, X., Peng, L., Qi, J., Yan, L., Zhang, Y., Zhao, H., Zheng, Y., He, K., and Zhang, Q.: Trends in China's anthropogenic emissions since 2010 as the consequence of clean air actions, Atmos. Chem. Phys., 18, 14095-14111, https://doi.org/10.5194/acp-18-14095-2018, 2018.